AAC
Journals.ASM.org

Miltefosine Increases Lipid and Protein Dynamics in *Leishmania amazonensis* Membranes at Concentrations Similar to Those Needed for Cytotoxicity Activity

Rodrigo Alves Moreira,[a] Sebastião Antonio Mendanha,[a] Kelly Souza Fernandes,[a] Grazzielle Guimaraes Matos,[b] Lais Alonso,[a] Miriam Leandro Dorta,[b] Antonio Alonso[a]

Instituto de Física, Universidade Federal de Goiás, Goiânia, GO, Brazil[a]; Instituto de Patologia Tropical e Saúde Publica, Departamento de Imunologia e Patologia Geral, Universidade Federal de Goiás, Goiânia, GO, Brazil[b]

Miltefosine (MT) is a membrane-active alkylphospholipid licensed for the topical treatment of breast cancer skin metastases and the oral treatment of leishmaniasis, although its mechanism of action remains unclear. Electron paramagnetic resonance (EPR) spectroscopy of a spin-labeled lipid and a thiol-specific spin label in the plasma membrane of *Leishmania* promastigotes showed that MT causes dramatic increases in membrane dynamics. Although these alterations can be detected using a spin-labeled lipid, our experimental results indicated that MT interacts predominantly with the protein component of the membrane. Cell lysis was also detected by analyzing the supernatants of centrifuged samples for the presence of spin-labeled membrane fragments and cytoplasmic proteins. Using a method for the rapid incorporation of MT into the membrane, these effects were measured immediately after treatment under the same range of MT concentrations that cause cell growth inhibition. Cytotoxicity, estimated via microscopic counting of living and dead cells, indicated ~70% cell death at the concentration of MT at which EPR spectroscopy detected a significant change in membrane dynamics. After this initial impact on the number of viable parasites, the processes of cell death and growth continued during the first 4 h of incubation. The EPR spectra of spin-labeled membrane-bound proteins were consistent with more expanded and solvent-exposed protein conformations, suggesting a detergent-like action. Thus, MT may form micelle-like structures around polypeptide chains, and proteins with a higher hydrophobicity may induce the penetration of hydrophilic groups of MT into the membrane, causing its rupture.

Leishmaniasis is caused by protozoan parasites of over 20 *Leishmania* species and is transmitted to humans via the bite of infected female sand flies. There are three main types of leishmaniasis: cutaneous (the most common form), visceral (the most severe clinical manifestation, which is fatal if untreated), and mucocutaneous. According to a recent report from the World Health Organization (WHO) (1), there are an estimated 1.3 million new cases of leishmaniasis worldwide and an estimated 20,000 to 30,000 deaths caused by these parasites annually.

Miltefosine (MT) was the first oral drug approved for use for the treatment of visceral and cutaneous leishmaniasis and is currently registered for leishmaniasis treatment in India (2002, as Impavido), Germany (2004), and Colombia (2005) (2). This drug is also used clinically for the topical treatment of skin metastases associated with breast cancer and cutaneous lymphoma (3). MT has shown high cure rates in the treatment of visceral (4), cutaneous (5), and mucocutaneous (6) leishmaniasis. Although many studies have been conducted to identify the mechanisms underlying the action of MT against tumor cells (3) and parasites (7), these mechanisms have not yet been determined. However, due to its chemical structure, which provides MT with a high membrane affinity, the primary molecular targets of MT are thought to be found at the level of the plasma membrane (3, 8, 9). As recently reported by Dorlo et al. (7), very similar mechanisms of action of MT against *Leishmania* parasites and human cancer cells have been identified, linking MT activity mainly to apoptosis resulting from the inhibition of phospholipid turnover and lipid-dependent cell signaling pathways (3, 7–9).

Electron paramagnetic resonance (EPR) spectroscopy of several fatty acid spin labels was recently employed to demonstrate that the application of MT at concentrations of up to 25 mol% in 1,2-dipalmitoyl-*sn*-glycero-3-phosphocholine (DPPC) vesicles subjected to a rigorous extrusion process does not alter vesicle lipid dynamics (10). Additionally, it was shown that MT causes remarkable increases in the lipid fluidity of stratum corneum membranes when measured directly in tissue but results in only a small alteration of lipid fluidity in a stratum corneum membrane model (10). MT also causes dramatic increases of membrane fluidity in erythrocyte ghost membranes and detergent-resistant membranes (DRMs) (11). In the present study, we further demonstrated that MT exerts a strong effect on the plasma membrane of *Leishmania amazonensis* promastigotes within the same MT concentration range that inhibits cell growth and causes lysis of the parasite. Moreover, an efficient method for the incorporation of MT into the *Leishmania* membrane allowed these effects to be detected with no incubation period.

MATERIALS AND METHODS

Chemicals. The spin labels 5-doxyl stearic acid (5-DSA) and 4-maleimido-1-oxyl-2,2,6,6-tetramethylpiperidine (6-MSL) (Fig. 1) were purchased from Sigma-Aldrich (St. Louis, MO). MT (Fig. 1) (molec-

Received 22 June 2013 Returned for modification 20 September 2013
Accepted 4 March 2014
Published ahead of print 10 March 2014
Address correspondence to Antonio Alonso, alonso@if.ufg.br.

doi:10.1128/AAC.01332-13

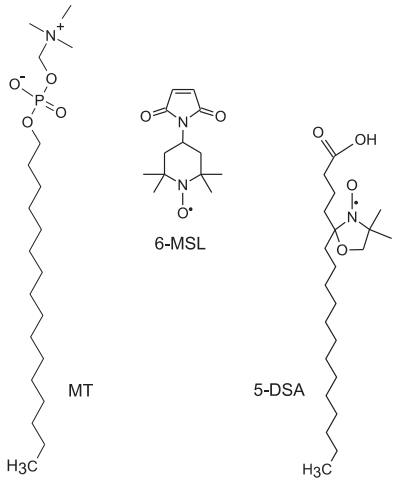

FIG 1 Chemical structures of MT and the spin labels 5-DSA and 6-MSL.

ular weight, 407.57) was purchased from Avanti Polar Lipids Inc. (Alabaster, AL).

Parasites. Promastigotes of *Leishmania* (*Leishmania*) *amazonensis* (MHOM/BR/75/Josefa) reference strains were grown in 24-well microtiter plates containing Grace's insect medium (Sigma-Aldrich) supplemented with 20% heat-inactivated fetal calf serum (FCS), 2 mM L-glutamine, 100 U/ml penicillin, and 100 μg/ml streptomycin (Sigma-Aldrich), as previously described (12).

Spin labeling and treatment with miltefosine. As described previously, the lipid spin labels were incorporated into the *Leishmania* membranes first by making films of the spin labels on the bottoms of test tubes (10, 11). A 1-μl aliquot of a stock solution of the spin label 5-DSA in ethanol (4 mg/ml) was transferred to a glass tube, and after solvent evaporation, 50 μl of a *Leishmania* suspension containing 10^8 cells in phosphate-buffered saline (PBS) was added to the spin-label film, followed by gentle agitation. Following spin labeling, a similar procedure was applied to treat the *Leishmania* promastigotes with MT (11). An aliquot (1 to 5 μl) of a stock solution of MT in ethanol (30 or 100 mg/ml) was used to generate a film in a glass tube at concentrations varying from 30 to 300 μg. Spin labeling of *Leishmania* membrane proteins was performed through incubation for 2 h at 26°C after the addition of an excess of the thiol-specific spin label 6-MSL. To remove the free spin label, the *Leishmania* suspension was centrifuged (5,000 × *g*, 4°C) for 15 min and then resuspended in PBS; this procedure was repeated 8 times. Each spin-labeled and treated sample was then introduced into a flame-sealed 1-mm (inner diameter) capillary tube for EPR measurements.

EPR spectroscopy. A Bruker ESP 300 spectrometer (Bruker, Rheinstetten, Germany) equipped with an ER 4102 ST resonator was used to perform the EPR measurements. The instrument parameters were as follows: microwave power, 2 mW; modulation frequency, 100 kHz; modulation amplitude, 1.0 G; magnetic field scan, 100 G; sweep time, 168 s; and detector time constant, 41 ms. All measurements were performed at 25 ± 1°C. EPR spectrum simulations were conducted using a nonlinear least-squares (NLLS) fitting program (13). In the spectral calculations, the NLLS program includes the magnetic g and A tensors and the rotational diffusion tensor (R), which are expressed in a system of Cartesian axes fixed on the spin-labeled molecule. To reduce the number of parameters in the fittings and simplify the simulation, the average rotational diffusion rate (R_{bar}) was calculated by the fitting program on the basis of the relationship $(R_{per} \cdot 2R_{par})^{1/3}$, where R_{per} is the perpendicular component and R_{par} is the parallel component of the rotational diffusion. R_{bar} was converted to the rotational correlation time (τ_c) parameter following the relationship $1/6(R_{bar})$ (13). Similar to previous studies (14, 15), the magnetic parameters were determined on the basis of a global analysis of the overall spectra obtained in this work, and all of the EPR spectra were simulated using the same magnetic parameters (g and A tensors).

Cell viability assay. To incorporate the MT into the *Leishmania* membranes, MT films were generated on the bottoms of test tubes, as previously described (10, 11). Following the treatment of *L. amazonensis* promastigotes with MT, cell viability and growth inhibition were assessed via microscopic counting of living and dead cells using the trypan blue exclusion method. Briefly, cells were resuspended in PBS or culture medium containing 10^8 cells/50 μl and treated with MT as described above for the EPR measurements (using MT films on the bottoms of glass tubes), and after 40-fold dilution, 0.1% (wt/vol) trypan blue (Sigma-Aldrich) was added. The living and dead cells in each sample were counted in a Neubauer chamber after a number of different incubation times (5 min and 1, 2, 4, and 24 h).

Cytotoxicity assay. Parasites at a concentration of 1×10^7 cells/ml in culture medium supplemented with 10% FCS were incubated for 24 h in 96-well culture dishes (Corning Life Sciences, Corning, NY) with increasing concentrations of MT (1 to 80 μM). We also performed experiments using different cell concentrations (2×10^7, 4×10^7, and 2×10^9 cells/ml) or incubation times (5 min and 1 h) and an FCS concentration of 20%. Cell viability was assessed by measuring the cleavage of 3-(4,5-dimethylthiazol-2-yl)-2,5-diphenyl tetrazolium bromide (MTT; Sigma-Aldrich) by metabolically active cells as described previously (16). Briefly, the parasites were incubated in a solution containing 5 mg/ml MTT for 3 h at 26°C, and the absorbance at 550 nm was read using a T80+ spectrophotometer (PG Instruments, Wibtoft, England). Measurements were performed in triplicate for each treatment, and the obtained values were used to calculate the mean percentage of viable cells relative to the number for the control. The 50% inhibitory concentration (IC_{50}) was then determined on the basis of a sigmoidal fitting (Boltzmann function) of the concentration-response curve. The mean IC_{50} and its standard deviation (SD) were obtained from at least three independent experiments.

Membrane disruption measurements. *Leishmania* membrane proteins were spin labeled and treated with MT as described above. Following treatment (1 to 5 min), the samples were centrifuged at 5,000 × *g* for 15 min at room temperature, and the supernatant was transferred to a capillary to check for the presence of spin-labeled membrane fragments via EPR spectroscopy. Alternatively, the protein content in the supernatant was measured using a commercial kit (Sigma) based on the bicinchoninic acid (BCA) reaction.

Statistical analysis. All data presented are expressed as the mean ± SD from at least three independent experiments. Data were compared via one-way analysis of variance (ANOVA), followed by Tukey's multiple-range test for statistically significant differences at a P value of <0.05.

RESULTS

MT increases the molecular dynamics of *Leishmania* membranes. The EPR spectra of the spin-labeled lipid 5-DSA (Fig. 1) incorporated into the plasma membranes of *Leishmania* promastigotes that were either subjected to MT treatment or not are shown in Fig. 2. Two dynamic parameters, τ_c and $2A_{//}$, indicated progressive increases in membrane fluidity with increasing MT concentration. τ_c is a motion parameter obtained from the spectral simulation, and $2A_{//}$ is a practice parameter measured directly in the EPR spectra that has been widely used to monitor membrane fluidity, although in principle, $2A_{//}$ is a static parameter associated with the orientational distribution of the spin label in the membrane (molecular order).

To examine the dynamic changes in the membrane protein component, the maleimide spin label 6-MSL (Fig. 1) was used. The EPR spectra of 6-MSL attached to the sulfhydryl groups in the membranes of *Leishmania* promastigotes either treated with MT or not are shown in Fig. 3. The spectra of the untreated samples showed a spectral line shape typical of proteins in general, with a

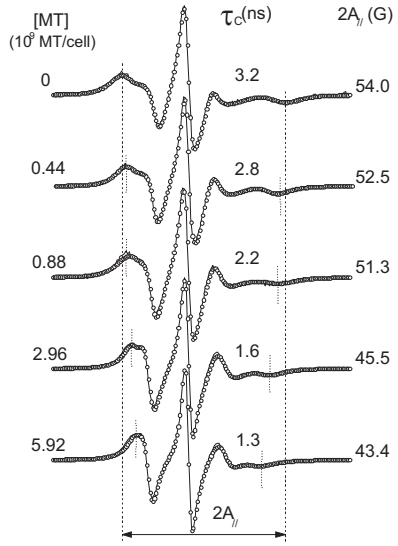

FIG 2 EPR spectra of 5-DSA in the plasma membranes of *Leishmania* cells with or without treatment with MT. The best-fit spectra (open circles) were provided by NLLS fitting using a two-component model for all fittings to obtain the average rotational correlation time, τ_c. The values of the EPR parameters τ_c and $2A_{//}$ are indicated, where $2A_{//}$ (outer hyperfine splitting) is the separation (in magnetic field units) between the first peak and the last inverted peak of the spectrum (indicated by vertical lines). These two parameters decrease with increases in membrane fluidity. The experimental errors obtained for τ_c and $2A_{//}$ are 0.2 ns and 0.5 G, respectively.

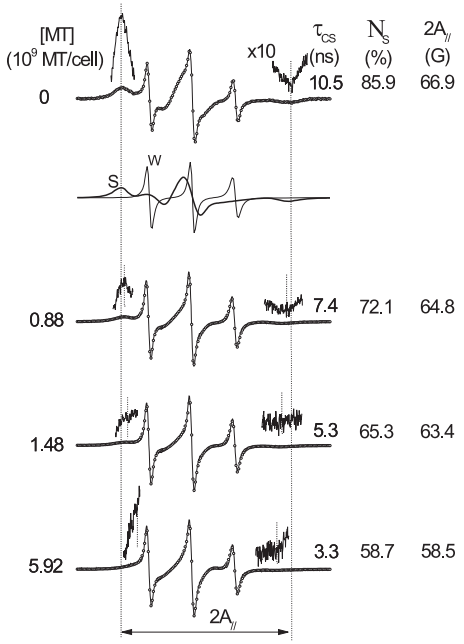

FIG 3 Experimental (full line) and best-fit (open circles) EPR spectra generated at 25°C for 6-MSL bound to the sulfhydryl groups of *Leishmania* membrane proteins in untreated and MT-treated samples. The best-fit spectra were obtained by NLLS fitting using a two-component model for all fittings. The spectra of the S and W components, which together form the simulated spectrum of the control sample (first spectrum), are indicated by thick (S component) and thin (W component) lines. The values of three EPR parameters are indicated: the rotational correlation time of the S component (τ_{cS}) and the population of the S component (N_S), which were generated by the fitting program, and $2A_{//}$, which was measured from the spectrum, as indicated by vertical lines. The regions corresponding to the first and last resonance lines in the spectrum were amplified 10 times to improve the visualization of their magnetic field positions.

$2A_{//}$ value of 67 G at 25°C. This value is similar to the values found for spin-labeled proteins in the stratum corneum (the outermost skin layer) (14, 15) and bovine serum albumin (BSA) spin labeled on its single sulfhydryl group (17). The EPR spectra of spin-labeled proteins are generally composed of two spectral components corresponding to two spin probe populations associated with two states of probe mobility, technically denoted strongly and weakly immobilized components (referred to here as the S and W components, respectively) (14, 15). Although spectroscopy of spin-labeled proteins has been widely employed to analyze protein structure via the site-directed spin-labeling method (18), the origin of the two spectral components is still not well understood. Our current interpretation has been described in previous work (17) and can be summarized as follows. The more mobile component, W, presents three sharp resonance lines with an isotropic hyperfine splitting ($2a_0$) equal to 17.1 G, consistent with a nitroxide moiety dissolved in buffer, whereas the less mobile component, S, exhibits a rotational correlation time approximately 1 order of magnitude greater than that of the W component, indicating strong interactions between the nitroxide side chain and the protein backbone. One interaction that contributes to the formation of the less mobile component, S, is hydrogen bonding between the nitroxide radical and any hydrogen donor in the protein, as deduced from the observed value of the *z* component of the ^{14}N-labeled hyperfine tensor (A_{zz}), which can be assessed by spectral simulation or through direct measurement at −140°C. Local electric fields can affect the unpaired electron density on the nitrogen nuclei and alter the parameter A_{zz} by modulating the Fermi contact interaction. When the nitroxide radical forms hydrogen bonds in a crystalline state, the A_{zz} value is approximately 35 G (19), and this value may decrease by approximately 3 G in a hydrophobic environment. Thus, the τ_c values of the W and S components reflect the dynamics of the spin-labeled side chain when the nitroxide moiety is either free in the solvent or tethered to the local polypeptide chain, respectively.

Increasing the MT concentration in the samples increased the polypeptide chain dynamics of the membrane-bound proteins, as indicated by the τ_c and $2A_{//}$ values of the S component (Fig. 3). The fast-motion EPR line shape (W component) displayed isotropic hyperfine splitting consistent with a nitroxide side chain being dissolved in an aqueous environment, indicating that the sulfhydryl groups of the membrane accessed by the spin label are essentially found in the outer layer of the membrane, where they are accessible to the aqueous solvent. If the nitroxide radical comes into contact with cytoplasm constituents, it would be reduced by ascorbic acid, Fe(II), or other reducing agents and, thus, become EPR silent. The presence of MT diminished the population of the S component (N_S), providing support for the notion that MT destabilizes membrane proteins, leading to more expanded and solvent-exposed conformations. The plots shown in Fig. 4 depict the effects of the MT concentration on the $2A_{//}$ values of both spin labels (5-DSA and 6-MSL) in the *Leishmania* membranes. A significant increase in the dynamics of both the lipid and protein spin labels was observed at a concentration as low as 0.44×10^9 MT molecules/cell.

Cell viability measurements. To examine how the changes in

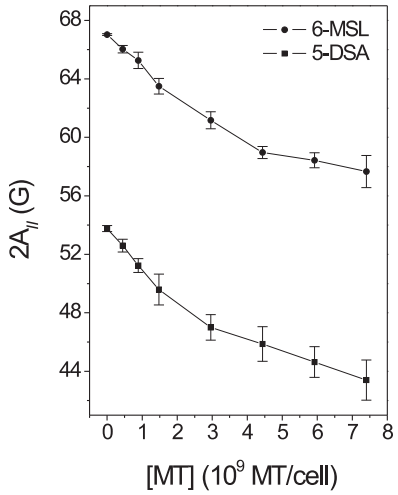

FIG 4 The EPR parameter $2A_{//}$ for the spin labels 5-DSA and 6-MSL in *Leishmania* membranes as a function of the MT concentration. The results for samples treated with MT at a concentration of 0.44×10^9 MT molecules/cell were significantly different from those for the control samples at a P value of <0.05 for both spin labels, and the results for all other samples were significantly different from those for the control at a P value of <0.01.

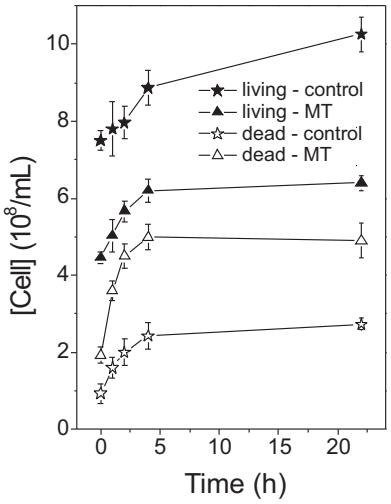

FIG 6 Numbers of living and dead cells in untreated *Leishmania* samples and those treated with MT (0.44×10^9 MT molecules/cell) in culture medium for several different incubation periods at 26°C. Concentrations of 0.89×10^9 and 1.48×10^9 MT molecules/cell showed similar effects (data not shown).

membrane dynamics affected the growth of the parasites, we counted the numbers of living and dead cells following treatment with MT. For cells treated in PBS, as in the EPR experiments, approximately 70% cell death was observed at the MT concentration that produced significant membrane alterations, as detected via EPR spectroscopy (Fig. 5). Similar experiments conducted in cells in culture medium supplemented with 10% FCS showed that to achieve 50% cell death, an MT concentration more than twice the concentration required in PBS was necessary, indicating that a considerable fraction of MT remains bound to the albumin present in FCS (Fig. 5). Cell counts recorded following several different periods of incubation at 26°C (Fig. 6) demonstrated that immediately after treatment with MT, a considerable fraction of the cells was killed, but the process of cell death and growth continued, especially in the first 4 h of incubation.

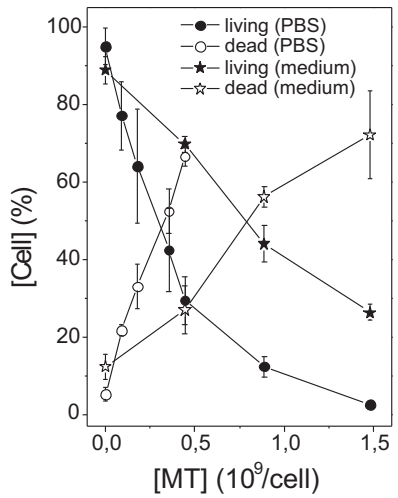

FIG 5 Cell counts for *Leishmania* samples treated with MT. Living and dead cells were counted via the trypan blue exclusion method 1 to 5 min after treatment of *L. amazonensis* promastigotes in PBS or culture medium.

Cytotoxicity assay. The cellular metabolic activity was also measured using the MTT cleavage assay, varying the cell and FCS concentrations and the period of incubation prior to the addition of MTT (Table 1). Our first three experiments using different concentrations of parasites showed that the IC_{50} values (μM) were increased when there were higher parasite concentrations in the samples. Thus, it seems to be more appropriate to express the IC_{50} as the number of molecules per cell, particularly in the case of MT, which shows a high affinity for membranes. The IC_{50} expressed as the number of MT molecules per parasite decreased with an increase in the cell concentration, which can be explained by the fact that the sample with the highest concentration of cells contained a lower concentration of albumin; i.e., a higher concentration of MT reached the membrane. When the experiment was performed with the same number of cells but twice the concentration of albumin (20% FCS), the IC_{50} values increased significantly. Reducing the incubation time prior to the addition of MTT led to an increase in IC_{50}s, indicating that the MT initially incorporated in albumin requires a long period to reach the parasite membrane. In contrast, when treatments were performed by placing a high concentration of cells over an MT film in a glass tube with moderate stirring, the incorporation of the drug into the cells was so rapid and efficient that the effect was observed after only 5 min of incubation.

***Leishmania* lysis induced by MT.** Cell lysis was also observed under the range of MT concentrations that alter *Leishmania* membrane fluidity. Soon after treatment with MT, the 6-MSL-labeled *Leishmania* cells were centrifuged and the EPR spectra of the supernatants were recorded. The EPR spectrum intensity increased with the MT concentration in the samples, reaching a plateau at a concentration of 1.48×10^9 MT molecules/cell (Fig. 7). The EPR spectra shown in Fig. 7 are for spin-labeled membrane fragments present in the supernatants of samples treated with MT and are similar to those presented in Fig. 3, which were obtained under higher MT concentrations. Untreated samples showed a weak

TABLE 1 *In vitro* activity of MT against *L. amazonensis* promastigotes[d]

No. of parasites/ml	Incubation time[a]	IC_{50} (μM)	MIC_{100} (μM)	IC_{50} (10^9 MT molecules/cell)
2×10^7	24 h	26.4 ± 6.4 (A)[d]	99.7 ± 24.7	0.79 ± 0.19 (A)
4×10^7	24 h	43.4 ± 8.9 (AB)	96.1 ± 14.3	0.65 ± 0.14 (AB)
1×10^8	24 h	59.3 ± 9.2 (B)	151.2 ± 31.0	0.36 ± 0.06 (BC)
1×10^8 (20% FCS[b])	24 h	126.2 ± 31.6 (C)	245.7 ± 59.0	0.76 ± 0.19 (A)
1×10^8	1 h	143.9 ± 19.4 (C)	218.41 ± 20.1	0.87 ± 0.12 (AB)
2×10^9 (film[c])	5 min			0.53 ± 0.12 (ABC)

[a] Incubation time after treatment and before MTT addition.
[b] The amount of fetal calf serum in the culture medium used was 20% instead of 10%.
[c] Method for rapid miltefosine incorporation (see Materials and Methods).
[d] For statistical significance, in each column, the data that are not indicated with capital letters in common are significantly different at a *P* value of <0.05. The statistical significance for MIC_{100} was the same as that for IC_{50}.

EPR signal, most likely because not all of the free spin label was removed from the samples during the preparation process. A plot of the EPR signal intensity versus the MT concentration in comparison with measurements of cell lysis based on the protein content in the supernatant is shown in Fig. 8. The observation that the EPR signal intensity remained stable at concentrations above 1.5×10^9 MT molecules/cell while the supernatant protein content was still increasing may have been caused by nitroxide reduction due to contact with cytoplasmic contents following cell lysis.

DISCUSSION

In this study, we used a method for achieving the rapid incorporation of MT into the membranes of *Leishmania* promastigotes to measure its effects on membrane dynamics and the inhibition of cell growth. This method for incorporating molecules into membranes was developed and has been widely applied in spin-labeling EPR spectroscopy to study cell membranes. It consists of dissolving the spin label in ethanol to prepare a film on the bottom of a glass tube through the evaporation of the solvent. When high concentrations of cells are added to this film of spin-labeled lipids and moderately agitated, monomers of the labeled molecules are transferred to their membranes. The efficiency of incorporation and the uniformity of the probe distribution throughout the membrane can be verified on the basis of the EPR spectra immediately after labeling. For instance, spin-labeled lipids have been successfully incorporated into stratum corneum membranes (20), cellular membranes of coffee root tip segments (21), *Trypanosoma cruzi* protozoans (22), and fibroblasts (23). EPR spectroscopy has identified the presence of two populations of spin labels differing in molecular dynamics in cell membranes (24). The first population, spin-labeled lipids with lower mobility, was associated with boundary lipids that contact membrane proteins, whereas the second population, which had higher mobility, was attributed to the spin labels located in the bulk bilayer phase (24). For cell membranes in general, only the spectral component corresponding to the spin label that contacts proteins appears in the EPR spectra of 5-DSA due to the high proportion of membrane-bound proteins. Thus, a lipid probe can also reflect the dynamics of the protein component. The fact that MT essentially does not alter the lipid dynamics of phospholipid bilayers at concentrations up to a 25 to 35% molar ratio, as shown in previous work (10, 11), suggests that these changes in *Leishmania* membranes caused by MT are due to its action on membrane proteins.

As demonstrated by spin-labeling EPR data, MT induces conformational changes in the protein backbone, causing denatur-

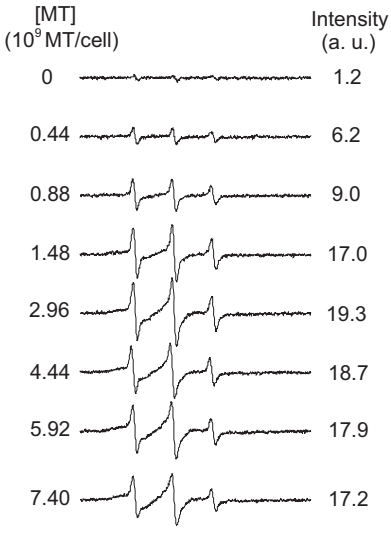

FIG 7 EPR spectra for the maleimide spin label 6-MSL covalently bound to the sulfhydryl groups of *Leishmania* membranes present in the supernatants of *Leishmania* samples treated with MT. With increases in the MT concentration, the samples showed increased contents of spin-labeled membrane fragments in the supernatant. a.u., arbitrary units.

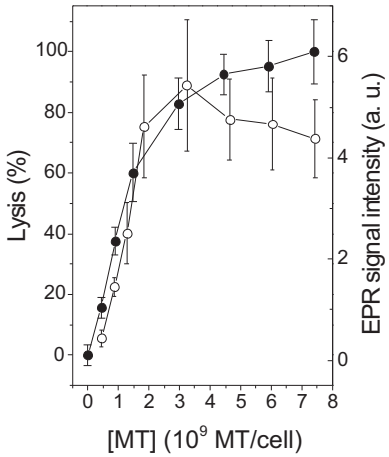

FIG 8 Percent cell lysis (closed circles) and content of spin-labeled membrane in the supernatant (open circles) in *Leishmania* samples treated with MT. Measurements of lysis were based on the protein contents in the supernatants of *Leishmania* samples.

ation at higher concentrations. In a recent study addressing the interaction of surfactants with BSA and employing the same technique, the spin label 5-MSL, which was covalently bound to the single free thiol group of this protein, showed that the surfactants cause a decrease in the EPR parameter $2A_{//}$ and the relative population of the S component, corresponding to more dynamic and solvent-exposed protein conformations (17). Among the models that have emerged to describe the structure of the protein-detergent complexes resulting from protein denaturation, the necklace-and-bead model is the most widely discussed in the literature (25). In this model, cooperative binding of surfactants induces the formation of necklace-and-bead-like structures in the unfolded protein, and the polypeptide chains wrap around micelle-like aggregates (25). A mechanism of MT action based on the indiscriminate attack of membrane-bound proteins is consistent with the wide-ranging activity of MT against pathogenic fungi (26), *Leishmania* species (7), *Trypanosoma cruzi* (27), and various types of tumor cells (3, 8).

The clinical pharmacokinetics of MT have been examined in patients with cutaneous leishmaniasis treated with 150 mg MT/day for 28 days: the median plasma MT concentration encountered during the last week of treatment was 30.8 μg/ml, with the concentration peaking at 51.6 μg/ml (28). In previous work, EPR measurements of spin-labeled erythrocyte membrane proteins have been performed directly in total blood to determine the minimum plasma MT concentration necessary to cause a change in protein dynamics. A significant effect was detected at 600 μg/ml, which was a concentration of MT that also caused 46% hemolysis (11). At the median and maximum MT plasma concentrations observed during the treatment of leishmaniasis (30.8 and 51.6 μg/ml, respectively) (28), a low level of hemolysis (2 to 3%) was also observed (11). The lower sensitivity of EPR spectroscopy relative to the sensitivity of the hemolytic potential may be because EPR is sensitive to a general change in the membrane, whereas the hemolytic effect depends on membrane rupture, which is a highly localized modification. Spin labels are sparsely distributed throughout the membrane, and to detect any alteration of membrane fluidity, a change in the environment of most spin probes, which requires a higher MT concentration, is necessary. In the present work, the changes detected in the membrane of *L. amazonensis* promastigotes occurred at MT concentrations very close to those that caused cell lysis (Fig. 8), antiproliferative activity (Fig. 5 and 6), and inhibition of parasite growth (Table 1).

It has been demonstrated that, at its IC_{50}, MT is able to induce programmed apoptosis-like cell death in *Leishmania donovani* (29, 30) and *L. amazonensis* (31) promastigotes. A comparison of our results regarding cell counts (Fig. 5 and 6) with the data reported by Verma et al. (30) is relevant in this context. These authors treated *L. donovani* promastigotes (5×10^6 cells/ml) with 25 μM MT (IC_{50}), and no effect of the drug was observed until at least 4 h after treatment. The cells treated with the drug had grown by approximately 50% after 12 h of treatment, and then their level remained constant up to 96 h, while untreated samples grew from 400 to 500% over the same period. An IC_{50} of 25 μM for 5×10^6 cells/ml is equivalent to 3×10^9 MT molecules/cell, which is approximately 3.8 times higher than the IC_{50} found in this study for *L. amazonensis* in culture medium (Fig. 5). The explanation for the higher drug/cell ratio may be associated with the low number of cells/ml used by Verma et al. (30); this number is commonly used but seems to be less similar to that encountered under physiological conditions. In human blood, MT must undergo partitioning over the membranes of all cells present in the blood and albumin, where there are approximately 5×10^9 erythrocytes/ml. The albumin/parasite ratio increases with the dilution of the parasites in the culture medium, which could result in delayed drug effects and increased IC_{50}s (Table 1 and Fig. 5). For *L. donovani* promastigotes, Paris et al. (29) found an IC_{50} of 13.6 μM, but as the authors used a concentration of 10^6 parasites/ml, this is equivalent to an IC_{50} of 8.16×10^9 MT molecules/cell, which is higher than the IC_{50} obtained by Verma et al. (30). Moreover, in their DNA fragmentation experiment, Paris et al. (29) applied 40 μM MT for 24 h. In the present study, a method for rapid drug incorporation into the membrane was employed to allow measurements to be made via EPR spectroscopy and microscopic counting of parasites without an incubation period. The data presented in Fig. 6 show that following treatment, there was a sharp drop in the number of parasites, though both their death and growth continued in the presence of MT. We believe that the parasites that received a lower concentration of the drug were those that were able to trigger programmed apoptosis-like cell death.

Interestingly, it has been demonstrated that MT exhibits not only *in vitro* antischistosomal activity but also *in vivo* activity with progressive membrane surface damage (32, 33). Additionally, tegumental damage was observed by scanning electron microscopy in the aquatic stages of schistosoma and its snail intermediate host after treatment with miltefosine (34). In a recent study highlighting *Giardia lamblia* as a possible new target for MT treatment, scanning and transmission electron microscopy revealed severe MT-induced morphological alterations in *G. lamblia* trophozoites, mainly at the level of the cell membrane and adhesive disc (35). MT also exhibits *in vitro* activity against *Trichomonas vaginalis* strains (36), clinical isolates of *Acanthamoeba* spp. (37), *Trypanosoma cruzi* (38), and *Streptococcus pneumoniae* (39) through attacking the plasma membrane and lytic activity in all cases.

In conclusion, MT exerted a strong impact on the plasma membranes of *Leishmania amazonensis* promastigotes, increasing the molecular dynamics of the membranes, as demonstrated using spin labels for lipid and protein components. The same range of MT concentrations also caused cell lysis and growth inhibition. The method applied for the rapid incorporation of MT into the membrane eliminated the false impression that MT requires a long incubation time to kill these parasites. However, the possibility that parasites are less affected by the MT triggering of programmed apoptosis-like cell death should not be ruled out. MT may penetrate the membrane via the lipid component and display a detergent-like activity at the lipid-protein interface, potentially nucleating micelle-like aggregates at hydrophobic sites in proteins and thereby destabilizing the proteins to promote more dynamic and expanded conformations. This interaction may further lead to membrane disruption due to penetration of the hydrophilic groups of MT into the interior of the membrane. A mechanism based on the indiscriminate attack of membrane-bound proteins is consistent with the reported broad spectrum of MT activity against pathogenic fungi and protozoa as well as some types of tumor cells. This work opens new perspectives to study and discover new drugs that have activity similar to that of MT but have a greater ability to selectively attack membrane proteins of *Leishmania* instead of the native cells.

ACKNOWLEDGMENTS

This work was financially supported by grants from the Brazilian research funding agencies CNPq, CAPES, FUNAPE, and FAPEG. Rodrigo Alves Moreira, Sebastião Antonio Mendanha, Kelly Souza Fernandes, Grazzielle Guimaraes Matos, and Lais Alonso are recipients of fellowships from CAPES. Antonio Alonso is the recipient of a research grant from CNPq.

We declare no conflicts of interest.

REFERENCES

1. **World Health Organization.** 2013. Leishmaniasis fact sheet no. 375. World Health Organization, Geneva, Switzerland. http://www.who.int/mediacentre/factsheets/fs375/en/.
2. **Olliaro PL, Guerin PJ, Gerstl S, Haaskjold AA, Rottingen J-A, Sundar S.** 2005. Treatment options for visceral leishmaniasis: a systematic review of clinical studies done in India, 1980-2004. Lancet Infect. Dis. **5:**763–774. http://dx.doi.org/10.1016/S1473-3099(05)70296-6.
3. **van Blitterswijk WJ, Verheij M.** 2008. Anticancer alkylphospholipids: mechanisms of action, cellular sensitivity and resistance, and clinical prospects. Curr. Pharm. Des. **14:**2061–2074. http://dx.doi.org/10.2174/138161208785294636.
4. **Bhattacharya SK, Sinha PK, Sundar S, Thakur CP, Jha TK, Pandey K, Das VR, Kumar N, Lal C, Verma N, Singh VP, Ranjan A, Verma RB, Anders G, Sindermann H, Ganguly NK.** 2007. Phase 4 trial of miltefosine for the treatment of Indian visceral leishmaniasis. J. Infect. Dis. **196:**591–598. http://dx.doi.org/10.1086/519690.
5. **Soto J, Arana BA, Toledo J, Rizzo N, Vega JC, Diaz A, Luz M, Gutierrez P, Arboleda M, Berman JD, Junge K, Engel J, Sindermann H.** 2004. Miltefosine for New World cutaneous leishmaniasis. Clin. Infect. Dis. **38:**1266–1272. http://dx.doi.org/10.1086/383321.
6. **Soto J, Toledo J, Valda L, Balderrama M, Rea I, Parra R, Ardiles J, Soto P, Gomez SA, Molleda F, Fuentelsaz C, Anders G, Sindermann H, Engel J, Berman J.** 2007. Treatment of Bolivian mucosal leishmaniasis with miltefosine. Clin. Infect. Dis. **44:**350–356. http://dx.doi.org/10.1086/510588.
7. **Dorlo TPC, Balasegaram M, Beijnen JH, de Vries PJ.** 2012. Miltefosine: a review of its pharmacology and therapeutic efficacy in the treatment of leishmaniasis. J. Antimicrob. Chemother. **67:**2576–2597. http://dx.doi.org/10.1093/jac/dks275.
8. **Ruiter GA, Zerp SF, Bartelink H, van Blitterswijk WJ, Verheij M.** 2003. Anti-cancer alkyl-lysophospholipids inhibit the phosphatidylinositol 3-kinase-Akt/PKB survival pathway. Anticancer Drugs **14:**167–173. http://dx.doi.org/10.1097/00001813-200302000-00011.
9. **Moreira W, Leprohon P, Ouellette M.** 2011. Tolerance to drug-induced cell death favours the acquisition of multidrug resistance in Leishmania. Cell Death Dis. **2:**e201. http://dx.doi.org/10.1038/cddis.2011.83.
10. **Alonso L, Mendanha SA, Marquezin CA, Berardi M, Ito AS, Acuña AU, Alonso A.** 2012. Interaction of miltefosine with intercellular membranes of stratum corneum and biomimetic lipid vesicles. Int. J. Pharm. **434:**391–398. http://dx.doi.org/10.1016/j.ijpharm.2012.06.006.
11. **Moreira RA, Mendanha SA, Hansen D, Alonso A.** 2013. Interaction of miltefosine with the lipid and protein components of the erythrocyte membrane. J. Pharm. Sci. **102:**1661–1669. http://dx.doi.org/10.1002/jps.23496.
12. **Oliveira MA, Pires Ada S, de Bastos RP, Lima GM, Pinto SA, Pereira LI, Pereira AJ, Abrahamsohn Ide A, Dorta ML, Ribeiro-Dias F.** 2010. Leishmania spp. parasite isolation through inoculation of patient biopsy macerates in interferon gamma knockout mice. Rev. Inst. Med. Trop. Sao Paulo **52:**83–88. http://dx.doi.org/10.1590/S0036-46652010000200004.
13. **Budil DE, Lee S, Saxena S, Freed JH.** 1996. Nonlinear-least-squares analysis of slow-motion EPR spectra in one and two dimensions using a modified Levenberg-Marquardt algorithm. J. Magn. Reson. **120:**155–189. http://dx.doi.org/10.1006/jmra.1996.0113.
14. **Alonso A, dos Santos WP, Leonor SJ, dos Santos JG, Tabak M.** 2001. Stratum corneum protein dynamics as evaluated by a spin-label maleimide derivative: effect of urea. Biophys. J. **81:**3566–3576. http://dx.doi.org/10.1016/S0006-3495(01)75987-5.
15. **Alonso A, Vasques da Silva J, Tabak M.** 2003. Hydration effects on the protein dynamics in stratum corneum as evaluated by EPR spectroscopy. Biochim. Biophys. Acta **1646:**32–41. http://dx.doi.org/10.1016/S1570-9639(02)00545-9.
16. **Miguel DC, Yokoyama-Yasunaka JKU, Andreoli WK, Mortara RA, Uliana SRB.** 2007. Tamoxifen is effective against Leishmania and induces a rapid alkalinization of parasitophorous vacuoles harbouring Leishmania (Leishmania) amazonensis amastigotes. J. Antimicrob. Chemother. **60:**526–534. http://dx.doi.org/10.1093/jac/dkm219.
17. **Anjos JLV, Santiago PS, Tabak M, Alonso A.** 2011. On the interaction of bovine serum albumin with ionic surfactants: temperature induced EPR changes of a maleimide nitroxide reflect local protein dynamics and probe solvent accessibility. Colloids Surf. B Biointerfaces **88:**463–470. http://dx.doi.org/10.1016/j.colsurfb.2011.07.030.
18. **McCoy J, Hubbell WL.** 2011. High-pressure EPR reveals conformational equilibria and volumetric properties of spin-labeled proteins. Proc. Natl. Acad. Sci. U. S. A. **108:**1331–1336. http://dx.doi.org/10.1073/pnas.1017877108.
19. **Tabak M, Alonso A, Nascimento OR.** 1983. Single crystal ESR studies of a nitroxide spin label. I. Determination of the G and A tensors. J. Chem. Phys. **79:**1176–1184.
20. **dos Anjos JLV, de Sousa D, III, Alonso A.** 2007. Effects of ethanol/L-menthol on the dynamics and partitioning of spin-labeled lipids in the stratum corneum. Eur. J. Pharm. Biopharm. **67:**406–412. http://dx.doi.org/10.1016/j.ejpb.2007.02.004.
21. **Alonso A, Queiroz CS, Magalhães AC.** 1997. Chilling stress leads to increased cell membrane rigidity in roots of coffee (Coffea arabica L.) seedlings. Biochim. Biophys. Acta **1323:**75–84. http://dx.doi.org/10.1016/S0005-2736(96)00177-0.
22. **Desoti VC, Lazarin-Bidóia D, Sudatti DB, Pereira RC, Alonso A, Ueda-Nakamura T, Dias BP, Jr, Nakamura CV, de Oliveira Silva S.** 2012. Trypanocidal action of (−)-elatol involves an oxidative stress triggered by mitochondria dysfunction. Mar. Drugs **10:**1631–1646. http://dx.doi.org/10.3390/md10081631.
23. **Mendanha SA, Moura SS, Anjos JLV, Valadares MC, Alonso A.** 2013. Toxicity of terpenes on fibroblast cells compared to their hemolytic potential and increase in erythrocyte membrane fluidity. Toxicol. In Vitro **27:**323–329. http://dx.doi.org/10.1016/j.tiv.2012.08.022.
24. **Jost PC, Griffith OH, Capaldi RA, Vanderkooi G.** 1973. Evidence for boundary lipid in membranes. Proc. Natl. Acad. Sci. U. S. A. **70:**480–484. http://dx.doi.org/10.1073/pnas.70.2.480.
25. **Turro NJ, Lei X-G, Ananthapadmanabhan KP, Aronson M.** 1995. Spectroscopic probe analysis of protein-surfactant interactions: the BSA/SDS system. Langmuir **11:**2525–2533. http://dx.doi.org/10.1021/la00007a035.
26. **Widmer F, Wright LC, Obando D, Handke R, Ganendren R, Ellis DH, Sorrell TC.** 2006. Hexadecylphosphocholine (miltefosine) has broad-spectrum fungicidal activity and is efficacious in a mouse model of cryptococcosis. Antimicrob. Agents Chemother. **50:**414–421. http://dx.doi.org/10.1128/AAC.50.2.414-421.2006.
27. **Croft SL, Seifert K, Duchêne M.** 2003. Antiprotozoal activities of phospholipid analogues. Mol. Biochem. Parasitol. **126:**165–172. http://dx.doi.org/10.1016/S0166-6851(02)00283-9.
28. **Dorlo TP, van Thiel PP, Huitema AD, Keizer RJ, de Vries HJ, Beijnen JH, de Vries PJ.** 2008. Pharmacokinetics of miltefosine in Old World cutaneous leishmaniasis patients. Antimicrob. Agents Chemother. **52:**2855–2860. http://dx.doi.org/10.1128/AAC.00014-08.
29. **Paris C, Loiseau PM, Bories C, Bréard J.** 2004. Miltefosine induces apoptosis-like death in Leishmania donovani Promastigotes. Antimicrob. Agents Chemother. **48:**852–859. http://dx.doi.org/10.1128/AAC.48.3.852-859.2004.
30. **Verma NK, Singh G, Dey CS.** 2007. Miltefosine induces apoptosis in arsenite-resistant Leishmania donovani promastigotes through mitochondrial dysfunction. Exp. Parasitol. **116:**1–13. http://dx.doi.org/10.1016/j.exppara.2006.10.007.
31. **Marinho FDA, Gonçalves KCD, de Oliveira SS, de Oliveira A-CDSC, Bellio M, d'Avila-Levy CM, dos Santos ALS, Branquinha MH.** 2011. Miltefosine induces programmed cell death in Leishmania amazonensis promastigotes. Mem. Inst. Oswaldo Cruz **106:**507–509. http://dx.doi.org/10.1590/S0074-02762011000400021.
32. **Bertão HG, Silva RAR, Padilha RJR, de Azevedo Albuquerque MCP, Rádis-Baptista G.** 2012. Ultrastructural analysis of miltefosine-induced surface membrane damage in adult Schistosoma mansoni BH strain worms. Parasitol. Res. **110:**2465–2473. http://dx.doi.org/10.1007/s00436-011-2786-5.
33. **Eissa MM, El Azzouni MZ, Amer EI, Baddour NM.** 2011. Miltefosine, a promising novel agent for Schistosomiasis mansoni. Int. J. Parasitol. **41:**235–242. http://dx.doi.org/10.1016/j.ijpara.2010.09.010.
34. **Eissa MM, El Bardicy S, Tadros M.** 2011. Bioactivity of miltefosine

against aquatic stages of Schistosoma mansoni, Schistosoma haematobium and their snail hosts, supported by scanning electron microscopy. Parasit. Vectors **4:**73. http://dx.doi.org/10.1186/1756-3305-4-73.
35. **Eissa M, Amer E.** 2012. Giardia lamblia: a new target for miltefosine. Int. J. Parasitol. **42:**443–452. http://dx.doi.org/10.1016/j.ijpara.2012.02.015.
36. **Blaha C, Duchêne M, Aspöck H, Walochnik J.** 2006. In vitro activity of hexadecylphosphocholine (miltefosine) against metronidazole-resistant and -susceptible strains of Trichomonas vaginalis. J. Antimicrob. Chemother. **57:**273–278. http://dx.doi.org/10.1093/jac/dki417.
37. **Seifert K, Duchêne M, Wernsdorfer WH, Kollaritsch H, Scheiner O, Wiedermann G, Hottkowitz T, Eibl H.** 2001. Effects of miltefosine and other alkylphosphocholines on human intestinal parasite Entamoeba histolytica. Antimicrob. Agents Chemother. **45:**1505–1510. http://dx.doi.org/10.1128/AAC.45.5.1505-1510.2001.
38. **Santa-Rita RM, Santos Barbosa H, Meirelles MDNSL, de Castro SL.** 2000. Effect of the alkyl-lysophospholipids on the proliferation and differentiation of Trypanosoma cruzi. Acta Trop. **75:**219–228. http://dx.doi.org/10.1016/S0001-706X(00)00052-8.
39. **Llull D, Rivas L, García E.** 2007. In vitro bactericidal activity of the antiprotozoal drug miltefosine against Streptococcus pneumoniae and other pathogenic streptococci. Antimicrob. Agents Chemother. **51:**1844–1848. http://dx.doi.org/10.1128/AAC.01428-06.